

Seafloor Kinematics of the Near-Greenland Region of the Eurasian Basin

A. A. Schreider^{a, *}, A. E. Sazhneva^a, M. S. Kluev^a, A. L. Brehovskii^a, I. Ya Rakitin^a, and O. A. Zuev^b

^a*Shirshov Institute of Oceanology, Russian Academy of Sciences, Moscow, 117218 Russia*

^b*Moscow Institute of Physics and Technology, Moscow, 141701 Russia*

**e-mail: aschr@ocean.ru*

Received November 24, 2015; revised March 3, 2016; accepted September 6, 2018

Abstract—The Lincoln Sea floor evolved during stretching of a segment of the continental Greenland – Barents Sea shelf. Prior to the onset of extension, the continental shallow-water Morris Jesup Rise and the Yermak Plateau were a single unit. During rifting, this single continental plateau broke apart, initiating propagation of the Gakkel mid-ocean ridge toward the Atlantic. The breakup continued for ~1.5 Ma, 35.3–33.7 Ma ago. The emplacement of numerous mafic dikes during rifting could have caused the high-amplitude magnetic anomalies on the single plateau. For the first time, the fracture geometry involved in the breakup of the continental crust has been reconstructed, the Euler poles and angle of rotation describing its kinematics have been determined, and the paleobathymetry on the flanks of the fracture have been reconstructed.

DOI: 10.1134/S0001437019020152

INTRODUCTION

One of the most important directions in studying the Arctic is clarifying problems on the paleogeodynamics of the Arctic Ocean [18]. Questions of the origin and tectonic development of the Arctic Ocean are debated in the literature to this day [2, 4, 9, 10, 12, 13, 16, 19, 26, 37, 51, 52, 61–63, 67, 70, etc.].

A particular role is played by studies of the Eurasian Basin, which hosts the Arctic Ocean's sole active Mid-Arctic Ridge, the main link of which is known in the literature as the Gakkel [7], Nansen [67, etc.], and Nansen–Gakkel [48, etc.] mid-ocean ridge.

For brevity and convenience, in the present study, we will refer to it as the Gakkel mid-ocean ridge or the Mid-Arctic Ridge.

The Eurasian Basin also includes a number of smaller basins and uplifts. The Nansen Basin is located between the spreading axis of the Mid-Arctic Ridge and the Eurasian shelf. The Sophia Basin is located between the Yermak Plateau and Spitsbergen. The Amundsen Basin (also known as the Fram Basin [48] and the Polar Abyssal Plain [39]) lies between the Lomonosov Ridge and the axis of the Mid-Arctic Ridge; this basin also hosts the Earth's North Pole. The Lincoln Sea Basin lies between the Morris Jesup (also spelled Morris Jesup [48]) Rise and the Lomonosov Ridge. The Mid-Arctic Ridge separates the Morris Jesup Rise and the Yermak Plateau (Fig. 1).

Geological and geophysical study of the near-Greenland region of the Eurasian Basin, including the areas of the Amundsen Basin, the Morris Jesup Rise,

the Lincoln Sea Basin, and contiguous areas of the Lomonosov Ridge, plays an important role in reconstructing the initial stage of the Eurasian Basin's formation. Studies by the international scientific community in the last 50 years has made it possible to obtain information on the morphology of the seafloor relief, the sedimentary cover, the crustal structure, and anomalous potential fields of the Lincoln Sea Basin and its contiguous areas. In addition, it should be noted that the ice cover of the Arctic Ocean, including the area near Greenland, hinders the collection of data on the geological structure of its seafloor. There is still doubt that the geological samples recovered by research vessels may be the products of ice drift. The ice conditions extremely limit the possibilities of obtaining deep-water drilling data. Therefore, comprehensive analysis of the available geological and geophysical data may answer a number of questions on the stages of its geological development, which is the aim of the present study. Note that this paper uses the most updated version of the geochronological scale [36] developed in [15].

SEAFLOOR MORPHOLOGY AND DEEP-WATER DRILLING DATA

The near-Greenland area of the Amundsen Basin in the Eurasian Basin of the Arctic Ocean has no clearcut, geographically substantiated boundaries. This study considers it to be within the sector of 79°–90° N, 0°–35° E. It was mentioned above that it hosts the Lincoln Sea (its basin), which is a marginal sea of the Arctic

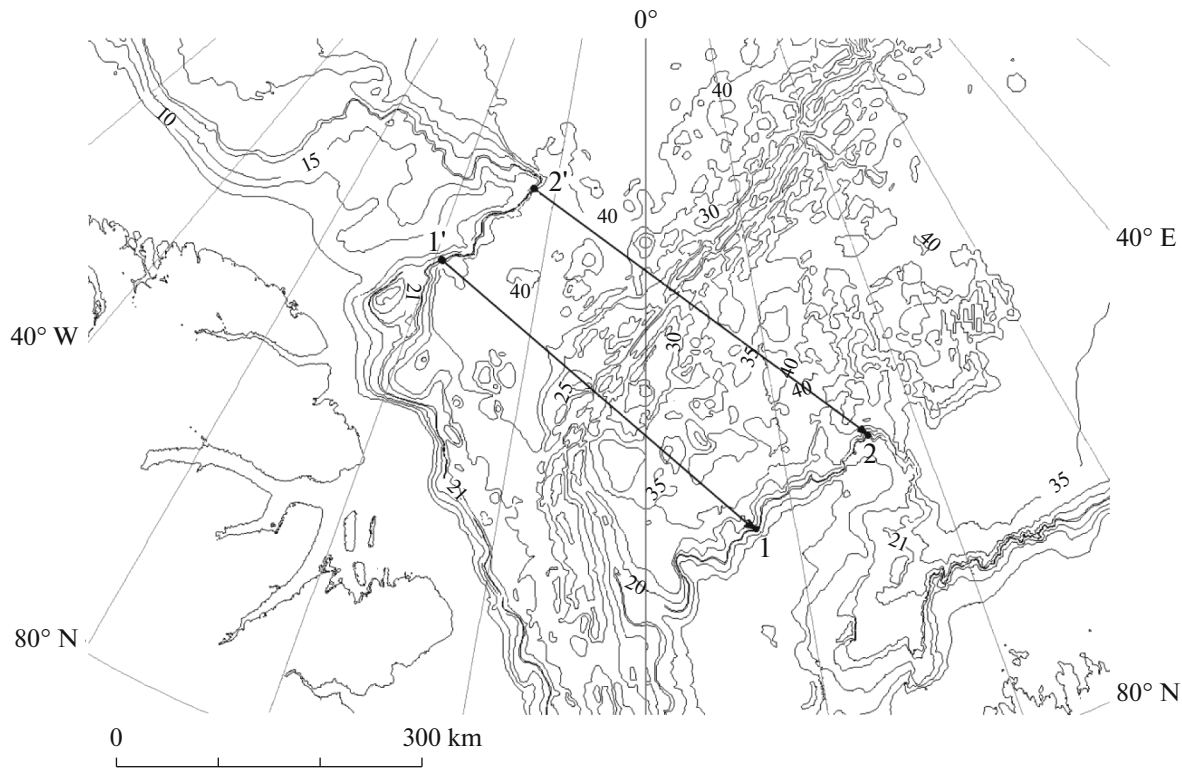


Fig. 1. Bathymetry of near-Greenland part of Eurasian Basin after data of [21]. Isobaths in hundreds of meters. The positions of endpoints of conjugate isobaths 1–2 of Morris Jesup Rise and 1'–2' of Yermak Plateau are shown; segments indicate lines of their alignment.

Ocean near the coasts of the islands of Ellesmere and Greenland. It occupies the northernmost position of all the Arctic seas and lies fully north of 80° N. It is bounded in the north by the conditional line between Cape Columbia (Ellesmere Island) and Cape Morris Jesup (Greenland); in the west and southwest, by the coast of Ellesmere Island; in the south, by the line between Cape Sheridan (Ellesmere Island) and Cape Bryant (Greenland); and in the southeast and south, by the Greenland coast. The seafloor depths (data of [21]) in the near-Greenland region of the Amundsen Basin exceed 3.5 km, whereas in the eastern Lincoln Sea, they do not surpass 2.5 km and gradually decrease to the west to 1 km or less. The mean width of the central part of the Lincoln Sea Basin is close to 150 km. The Morris Jesup Rise has mean surface depths of 1–2 km and a width of up to 100 km.

In the polar region of the Lomonosov Ridge, the 2004 ACEX expedition drilled five boreholes (M0002A, M0003A, M0004A, M0004B, and M0004C), which exposed an Upper Cretaceous–Holocene section of the sedimentary sequence. Based on a study of cores from boreholes M0002A (87°52.2' N, 139°19.1' E) and M0004A (87°52' N, 139°10' E) (Fig. 2a), a combined section was compiled with a thickness of 428 m and four lithostratigraphic complexes were identified, U1–U4 [20, 55].

Palynological data provide evidence for a Campanian age (~80 Ma ago) for the oldest U4 deposits recovered by drilling [20]. The sediment material in the boreholes is represented by [8, 14, 20] brown, olive-colored, gray, and black silts, silty clays, and clayey silts with colorful interlayers and lenses of sand. The available microfossil data point to a subtropical climate that existed at the end of the Paleocene – beginning of the Eocene in the polar area of the present-day Lomonosov Ridge with an average annual surface-water temperature of ~20°C in the basin.

For the first time, the drilling results [8, 14, 20] have yielded data on large-scale erosion in the polar area of the Lomonosov Ridge, which spanned the Maastrichtian–Early Paleocene, preceding Cenozoic sediment accumulation. In the combined sequence of the sedimentary cover on the Lomonosov Ridge, a hiatus was established at a depth of ~200 m within the sub-complex U1/6 (Middle Miocene–Middle Eocene), indicating missing deposits from this age interval in the stratigraphic sequence.

ANOMALOUS GRAVITY FIELD

The anomalous free-air gravity field [24, 25, 53, 54] is characterized by the presence of positive anomalies with an absolute value of up to 50–150 mgl,

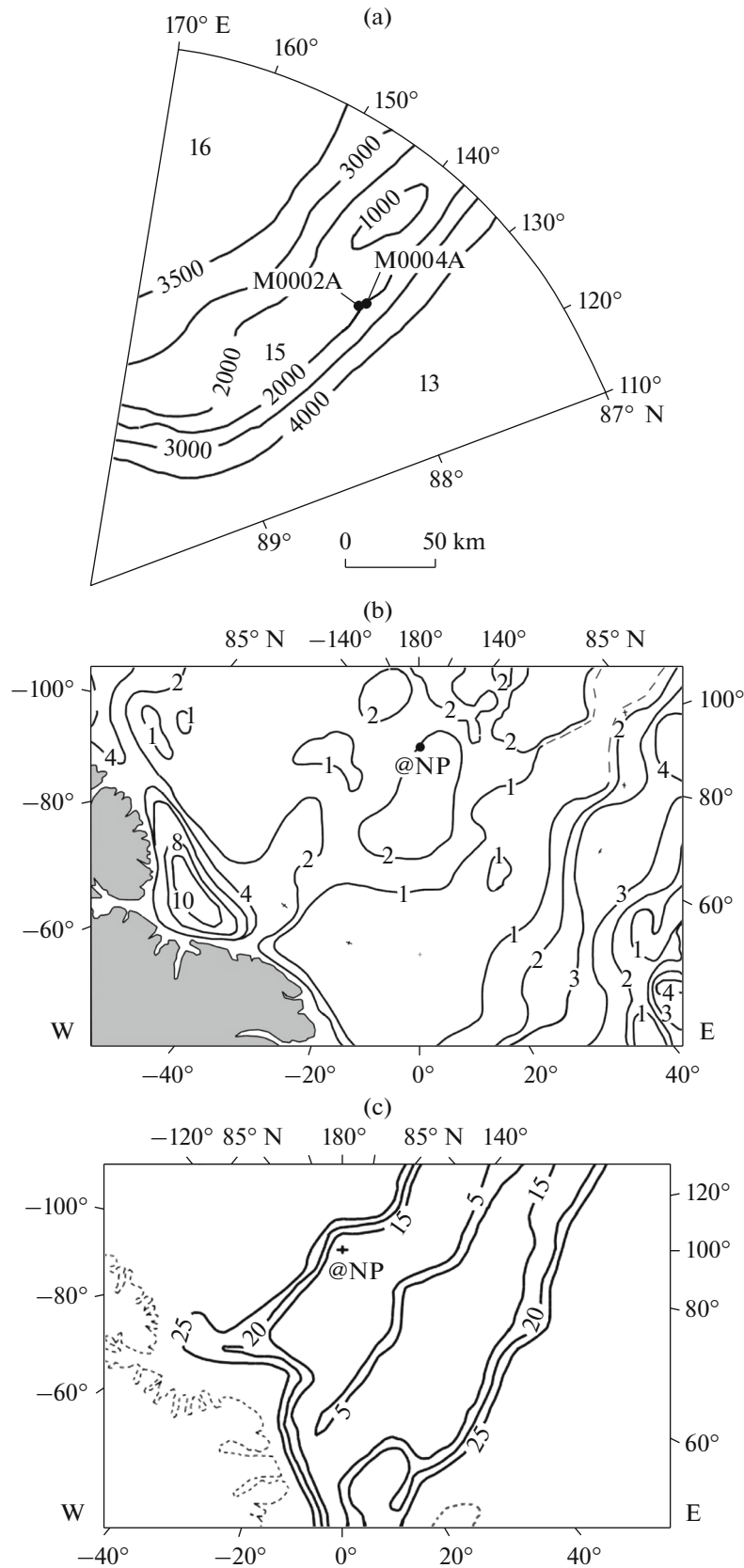


Fig. 2. Positions of deep-water drilling points (a) after data of [20, 55]; compilation scheme of sediment thickness (b) after data of [8, 11, 14, 19, 29, 38, 41, 49, 50, 57, 59, 61, 65, etc.] and thickness of Earth's crust (c) after data of [3, 19, 41, 45, 57, 59, 65]. Isopachous lines in km.

related to rises in the seafloor water area. Negative anomalies with an absolute value of up to -80 mgl are related to seafloor basins, well known in the literature.

The anomalous Bouguer gravity field was calculated from the IBACO seafloor relief database [21] and free-air gravity values with an intermediate layer density of 2.85 g/cm³ [54]. Its distribution is characterized by the presence of positive anomalies with an absolute value of up to 240 mgl, related to seafloor basins. Negative anomalies with an absolute value up to -70 mgl are related to islands and continental shelves. Here, the Morris Jesup Rise and the Yermak Plateau are characterized mainly by a weakly anomalous field with absolute values of gravity close to zero (sometimes with local extrema of up to 50 mgl).

According to [56, 65, etc.], in the central part of the Amundsen Basin, at depths of 4.1 – 4.2 km, for lithosphere with an age of 43 – 50 Ma, the heat flux values range from 73 to 127 mW/m², averaging 102 ± 12 mW/m² based on eight values. The obtained measurement data point to an increased heat flux compared to its mean oceanic values, which are close to 50 mW/m². The latter may reflect the closeness of the studied areas of the Amundsen Basin, which are separated by 100 – 200 km from the present-day active spreading axis of the Mid-Arctic Ridge in the Eurasian Basin of the Arctic Ocean. The tectonic activity of the seafloor in the near-Greenland region of the Amundsen Basin is also manifested as part of its seismic activity. Shallow-focus earthquakes with magnitudes of 4 – 5 s and source depths not exceeding 25 km are known in the Lincoln Sea (data of [1, 71]).

STRUCTURE OF THE UNCONSOLIDATED CRUST

In recent years, a certain number of studies have been conducted in the studied area employing point seismic sounding and continuous seismic profiling to investigate the sedimentary sequence and underlying layers of consolidated crust. The total length of the seismic profiles exceeds 6000 km. The present work is based on CDP materials along the drift lines of “North Pole” stations: NP-21 (1973), NP-24 (1978–1980), as well as on CDP profiles obtained by the R/V *Polarstern* in 1991 and 1998 and CDP profile 20010300 obtained by the *Polarstern* in 2001 [42–44]. These data have been synthesized in many aspects in [8, 14, 50].

Seismic stratigraphic study of the upper part of the crust on the Lomonosov Ridge has revealed sediments of several seismic complexes, the numbering and abbreviations of which differ based on the specifics of the studies. Different styles of sediment identification for the same areas have also been noted.

Thus, in [8, 43], along CDP profile 91090, the sediment layers nearest the surface (LR, Lomonosov Ridge) include [43] seismic complexes LR6 (0.08 – 0.1 km thick), LR5 (0.12 – 0.15 km thick), and LR4

(0.12 km thick). In [8], they are combined into the single seismic complex LR7 with *P*-wave velocities of 1.8 – 2.0 km/s. The L3 layer beneath them (0.11 – 0.15 km thick), with *P*-wave velocities of 2.2 km/s [43], is denoted as seismic complex LR6 in [8]. Below this lie seismic complexes LR5–LR4 [8], which combine sediment erosion material. Beneath these [43] are layers LR2 (0.55 – 0.83 km thick) and LR1 (0.84 – 1.65 km thick), with *P*-wave velocities of 4.0 – 4.6 km/s and 4.7 – 5.2 km/s, respectively. They are combined into seismic complex LR3–LR1 [8].

From this it is clear that the stratigraphic representation of sediments along the profile has no uniform nomenclature. In addition, the available material has made it possible to present a new map of the total thickness of the sedimentary layer (Fig. 2b) that integrates all available mapping (including profile) results of studying the sedimentary cover of the Eurasian Basin [8, 11, 14, 19, 29, 38, 41, 49, 50, 57, 59, 60, 65, etc.]. According to this new map, the sediment thickness near the foot of the Gakkel Ridge is around 1 km or less. In the polar area of the Amundsen Basin, it increases up to 3 km, whereas closer to the Lomonosov Ridge, it does not exceed 2 km. The trend of isopachous lines mainly follows the configuration of the basin. It is important to note that in the area of the Lincoln Sea, the sediment thickness increases and south of 85° N it reaches 9 – 12 km.

STRUCTURE OF THE ACOUSTIC BASEMENT

The sole of the sedimentary layer in the near-Greenland part of the Eurasian Basin is characterized by an irregular relief with a relative amplitude of individual forms of many hundreds of meters. Seismic studies using reflected waves and wide-angle seismic profiling indicate that the acoustic basement underlying the sediments is characterized by the presence of multiple faults, along which some of its blocks moved relative to others (e.g., [38, 41, etc.]). The basement is highly compartmentalized [14, etc.] with a complex internal structure [65, etc.] and reflectors, mainly in the depth interval of 4 – 9 s (two-way travel time).

The available material make it possible to present a new map of the total thickness of the crust (Fig. 2c) that integrates all available mapping (including profile) results of studying the continental and oceanic crustal layers of the Eurasian Basin [3, 19, 38, 41, 45, 59, 65, etc.]. Analysis of this new map makes it possible to characterize the composition and geometry of crustal layers.

In areas where continental crust has developed, the reflectors pertaining to the granite layer have seismic velocities close to 6.2 km/s. In areas where oceanic crust has developed, the velocities at comparable depths in the crust are close to 7 km/s and correspond to the basalt layer. It was possible to obtain a complete section of the crust at 5 seismic sounding points SB

(30, 31, 39, 48, 50) [29, 54]. At these points, mantle rocks have *P*-wave velocities of 8.2 km/s. In spreading areas of oceanic crust, the sole of the crust lies at depths close to 10 km, while in spreading areas of continental crust, the sole lies deeper than 30 km.

ANOMALOUS MAGNETIC FIELD

Aeromagnetic observations [26, 63, 67, etc.] have made it possible to obtain fundamental information on the distribution of magnetic anomalies in the near-Greenland area of the Eurasian Basin. According to this information, the Mid-Arctic Ridge, including the axial spreading zone, is characterized by low-amplitude linear magnetic anomalies (less than 500 nT) with a wavelength of up to 30 km. The axial magnetic anomaly reaches 2000 nT only in the west of the ridge and becomes significantly low in amplitude in almost all other areas. Comparison of the observed and theoretical magnetic anomalies in the seafloor spreading model has made it possible to identify linear magnetic anomalies C1–C25, which are associated with spreading.

In [47], paleomagnetic anomalies were identified for the ridge, the behavior of which differs from that discussed in [7] by the absence of transform faults. Note that study [46] recorded a high-amplitude shift in the spreading axis in the vicinity of 60° E. The most ancient anomaly has the number C24 [68], C24A, or even C24B [66]. In addition, studies [16, 47] identified areas with paleoanomaly C25. In the latter work, the paleoanomalies themselves in the Nansen Basin were traced to a large area in the direction of Spitsbergen.

Certain studies have observed the continental continuation of a number of linear magnetic anomalies. Thus, the linear anomalies from the Nansen Basin (e.g., a nameless paleoanomaly from [68] or anomaly 20 from [31]) cross to the eastern part of the Yermak Plateau. Linear magnetic anomaly C13 in [39] and C20 in [31] from the Amundsen Basin cross to the Morris Jesup Rise.

The magnetic field in the Lincoln Sea has been intensively studied in recent decades. In a number of works (e.g., [35, 46]), elongated magnetic anomalies have been distinguished on the continental slope and shelf of the sea; other studies show that south of 85.5° N, there are no paleomagnetic anomalies [16, 28, 31, 57, 62, etc.].

There are studies (e.g., [31, etc.]) that compare the observed and theoretical anomalies in the seafloor spreading model for the magnetic field of the basin north of 85.5° N. Based on the comparison, polarity chrons C18y–C24Bo have been identified, and in [16, 22], even C25o.

Similar studies that model paleomagnetic anomalies southeast of the Morris Jesup Rise have made it possible to identify paleoanomalies C1–C13. However, e.g., near the southeastern foot of the Morris

Jesup Rise, linear magnetic anomaly C13 from [62, 68] coincides with paleoanomalies C7 from [39].

All of the above indicates a lack of consistency in identifying linear magnetic anomalies and the polarity chrons responsible for them.

Therefore, it should be noted that the electronic database compiled by the authors of this article contains data on an aeromagnetic survey in 1998–1999 carried out by the United States Naval Research Laboratory (NRL) for the western half of the Eurasian Basin, which were published in 2003 [22]. The authors employed the survey results of the LOMGRAV-09 project published in [27], as well as the results of studies under the NOGRAM-99, NOGRAM 99-HELI, and NOGRAM00 programs. These surveys were carried out at an average flight altitude of 600 m.

Analysis of the data from these surveys along specific observational profiles does not confirm the presence of magnetic anomalies stretching tens of kilometers in the Lincoln Sea south of 85.5° N, nor does it allow us to reliably identify any linear magnetic anomalies associated with spreading in the Lincoln Sea or in the area of the Morris Jesup Rise. This, together with the results of seismic and gravimetric studies mentioned above, points to the continental nature of the lithosphere of the Morris Jesup Rise and Lincoln Sea south of 85° N.

Figure 3 shows the magnetic chronology of the seafloor of the near-Greenland area of the Eurasian Basin, as well as observed and theoretical magnetic anomalies in the inversion magnetoactive layer. In addition to the chrons known in the literature, the diagram in Fig. 3 includes the results of their refinement and partial reinterpretation in the region west of the Morris Jesup Rise.

Calculations of the spreading rates indicate that in the chron interval C25p–C13o, seafloor spreading proceeded at rates of ~0.85–1.5 cm/yr. In the chron interval younger than C13y, they decreased and the rate of opening does not exceed 0.8 cm/yr with an overall decrease in the spreading rates to the east. These circumstances hinder the reliable identification of specific paleoanomalies (their magnitude seldom exceeds 50–100 nT) and requires the identification of trains of chrons and their related paleomagnetic anomalies (e.g., C4–C5; C17–C18; etc.).

Analysis of paleomagnetic anomalies indicates that chron I2o is the closest to the eastern slope of the Morris Jesup rise from the Amundsen Basin side. Chron I5y approaches the northernmost cape of the rise (in both cases, the data of [22] were used).

DISCUSSION

The comprehensive interpretation of the geological and geophysical data indicates that the Morris Jesup Rise and the Yermak Plateau are a fragment that detached from the Eurasian continent during the for-

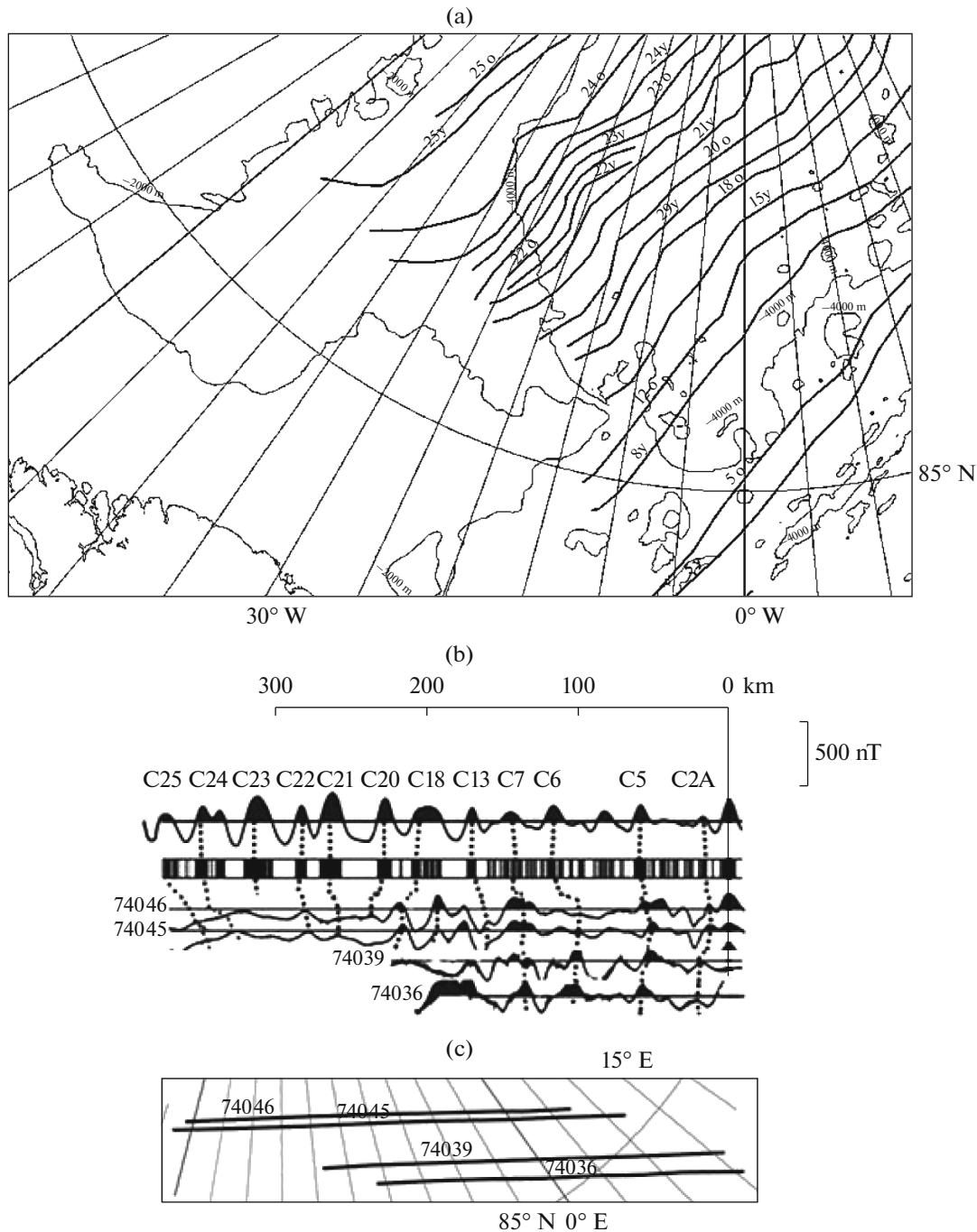


Fig. 3. (a) Age chrons of lithosphere; (b) theoretical paleoanomalies in inversion magnetoactive layer model and correlation of paleoanomalies C13–C25 along profiles 74036, 74039, 74045, and 74046, positions of which are shown in inset (c). Compiled from data of [16, 22, 27, 29] using geological scale from [36].

mation of the Eurasian Basin [30, 33, 34, 42]. This was most likely preceded by significant stretching of the continental crust in the junction area of Spitsbergen and the Morris Jesup–Yermak plateau. In this context, the existence of spreading-related linear magnetic anomalies on the continental Morris Jesup–Yermak plateau seems impossible. Therefore, we were forced to

refute the identification of paleomagnetic anomalies within their margins presented, e.g., in [31, 67, 68, etc.].

Analysis of these data along the observational profiles from [22], as well as the profile from [27], does not allow us, following [22], to reliably identify any linear magnetic anomalies in the Lincoln Sea. These are our grounds for suggesting the first reconstruction

of the fracturing involved in the breakup of the once unified Morris Jesup–Yermak continental plateau.

CALCULATION OF THE SPLITTING PARAMETERS

In the present work, the Bullard technique [23] is applied for the first time to align the continental slopes of the Yermak Plateau and the Morris Jesup Rise in the Eurasian Basin of the Arctic Ocean. Numerous tests for the compatibility of different areas of different and same-named isobaths have shown that the most suitable for the purposes of paleogeodynamic analysis were isobath areas in the range of 1.9–2.2 km. The slope in this depth interval is the steepest (the mean angle of inclination of the slope surface exceeds 7°) and, based on the data of [5] on the character of subsidence of the sediment sequence, it has the smallest sediment thickness (or is even completely devoid of sediment).

The Euler poles and angles of rotation were calculated with original software of the Laboratory of Geophysics and Tectonics of the Floor of the World Ocean, Shirshov Institute of Oceanology (IO RAS), incorporated into the Global Mapper program [17], the calculation principles of which are explained in [6]. For brevity, we call the isobath areas of opposite slopes conjugate.

If the breakup of the once unified Morris Jesup–Yermak massif, in accordance with the Wernicke scheme [69], is related to slipping of the Morris Jesup block of continental crust along the periphery of the Yermak, then the numerous tests for the compatibility of different areas of different and same-named isobaths have shown that the most suitable for paleogeodynamic analysis were isobath areas in the range of 1.8–2.3 km.

According to the calculated estimates, for a Euler pole of finite rotation at a point with coordinates 73.36° N, 23.56° W, it is possible over an extent of more than 130 km to obtain (Fig. 4) quite good alignment of the 2.0 km isobath of the Yermak slope (the area between points 1–2 in Fig. 1) and the 2.1 km isobath of the Morris Jesup slope (the area between points 1'–2' in Fig. 1). The angle of rotation was $8.1^\circ \pm 0.8^\circ$. Here, the standard deviation at the calculated alignment points was ± 7 km (seven alignment points).

Thus, as a result of these calculations, we reconstructed the axis of the splitting zone of the once joined Morris Jesup–Yermak continental plateau (thick line in Fig. 5). An important element in the reconstruction is identification of differences of hundreds of meters in the depths of the aligned isobaths. Based on this reconstruction, by introducing corrections for slipping of the above-mentioned fragments, we can reconstruct the primary paleobathymetry of the seafloor before the splitting of these sliding fragments (Fig. 6).

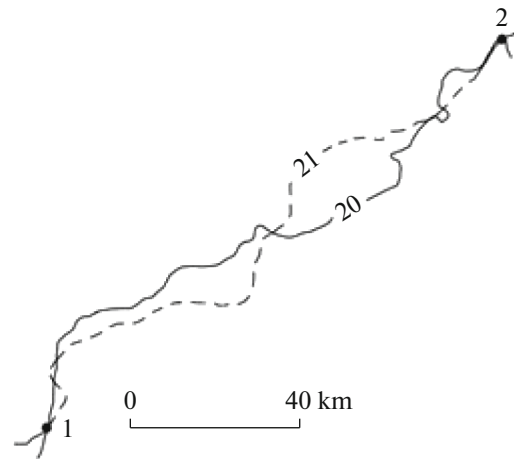


Fig. 4. Alignment of conjugate segments of isobaths of Morris Jesup Rise (2.1 km isobath, dotted line) and Yermak Plateau (2.0 km isobath, solid line). Points 1–2 are same as in Fig. 1.

It is clear from these figures that the initially peripheral areas of the Morris Jesup plateau rose above the main surface of the Yermak shelf by no more than a hundred meters.

Our parameters for the opening presented above make it possible to reconstruct the geometry of splitting between the Morris Jesup Rise and the Yermak Plateau, but they bear no information on the time thereof. Meanwhile, the data in Fig. 4 indicate that the oldest chron near the foot of the Morris Jesup Rise from the Yermak Plateau side has been dated as C12o. The chron at the foot of the Yermak Plateau also is known to be similarly dated [16, 22]. At the same time, chron C15o has been observed in immediate proximity to the northernmost submarine cape of the Morris Jesup Rise. This suggests that breakup of the continental crust along our reconstructed splitting occurred in the chron interval C15o–C13y (35.294–33.705 Ma ago), and regular spreading commenced in the chron interval C12o–C13y (33.705–33.157 Ma ago) and has continued to the present. The Euler poles describing the regular spreading are concentrated in the range 63° – 73° N, 129° – 145° E (data of [4, 32, 58, 64, etc.]). Therefore, the breakup process of the once joined Morris Jesup–Yermak plateau continued for ~ 1.5 Ma, 35.3–33.7 Ma ago.

CONCLUSIONS

Thus, as a result of our research, we found that the lithosphere of the Lincoln Sea formed during stretching of the continental Greenland–Barents Sea shelf. Prior to stretching, the continental shallow-water Morris Jesup Rise and the Yermak Plateau were a single unit. During rifting of the shelf, this single continental plateau broke apart, initiating propagation of the Gakkel mid-ocean ridge south toward the Atlantic.

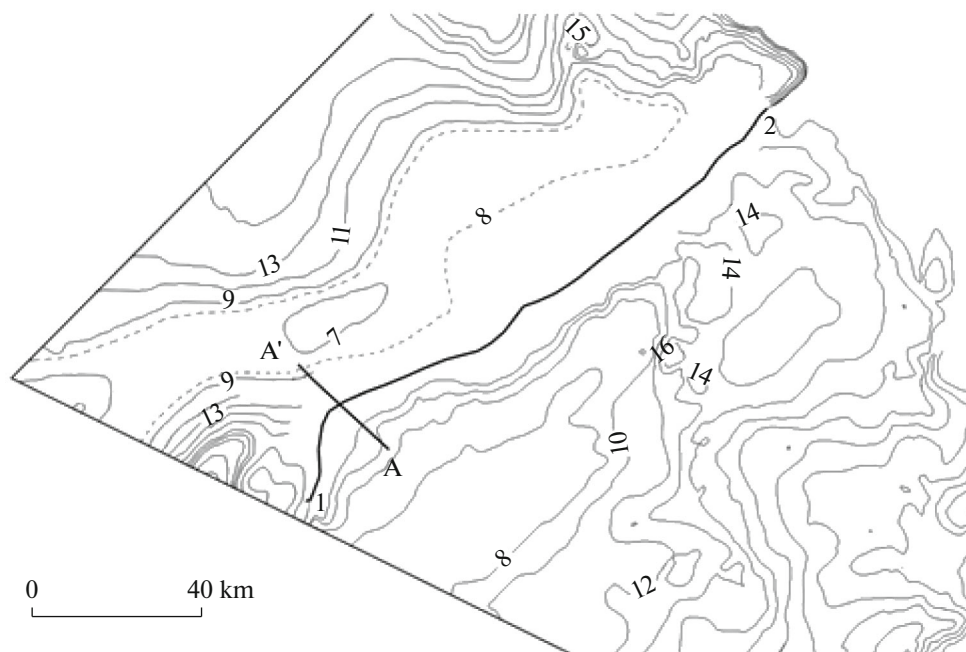


Fig. 5. Paleogeodynamic reconstruction of closing of opposite slopes of Morris Jesup Rise and Yermak Plateau based on conjugate isobaths and reconstructed paleobathymetry. Axis of splitting is shown (segment of thick curved line). Points 1–2 are same as in Fig. 1.

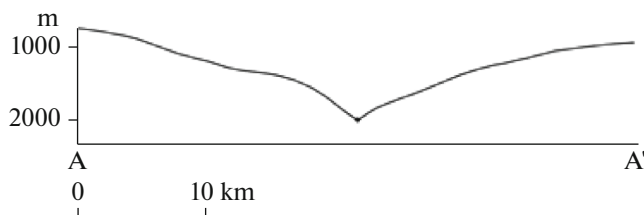


Fig. 6. Paleobathymetry profile along lines A¹–A in Fig. 5 before breakup of unified Morris Jesup–Yermak continental plateau.

The breakup process continued for ~1.5 Ma, 35.3–33.7 Ma ago. The emplacement of numerous mafic dikes in the rifting process could have caused the high-amplitude magnetic anomalies on the single plateau. For the first time, the fracture geometry involved in the breakup of the continental crust has been reconstructed, the Euler poles and angles of rotation describing its kinematics have been determined, and the paleobathymetry on the flanks of the fracture have been reconstructed.

FUNDING

The study was performed under State Assignment topic no. 0149-2019-0005. Methodological problems on the alignment of conjugate isobaths were solved within the framework of project no. 17-05-00075 of the Russian Foundation for Basic Research.

REFERENCES

1. G. P. Avetisov, "Seismic Arctic studies at the Scientific Research Institute of Geology of the Arctic–All-Russian Scientific and Research Institute of Geology and Mineral Resources of the World Ocean: history, achievements, and prospects," *Probl. Arkt. Antarkt.*, No. 2, 27–41 (2009).
2. N. A. Bogdanov, "Tectonics of the Arctic Ocean," *Geotectonics* **38**, 166–181 (2004).
3. A. N. Vinogradov, M. L. Verba, and F. P. Mitrofanov, "Reconstruction of evolution and modeling of riftogenic-collision systems of Euro-Arctic region," in *Fundamentals of Modern Strategy of Nature Management in Euro-Arctic Region* (Kola Scientific Center, Russian Academy of Sciences, Apatity, 2005), pp. 16–39.
4. V. Yu. Glebovsky, V. D. Kaminsky, A. N. Minakov, S. A. Merkur'ev, V. A. Childers, and J. M. Brozena, "Formation of the Eurasia Basin in the Arctic Ocean as inferred from geohistorical analysis of the anomalous magnetic field," *Geotectonics* **40**, 263–281 (2006).
5. V. V. Zhmur, D. A. Sapov, I. D. Nechaev, et al., "Intensive gravity currents in the near-bottom layer of the ocean," *Izv. Akad. Nauk, Ser. Fiz.* **66**, 1721–1726 (2002).
6. D. D. Zonenshain, M. G. Lomize, and A. G. Ryabukhin, *Practical Manual on Geotectonics* (Moscow State Univ., Moscow, 1990) [in Russian].
7. A. M. Karasik, "Geohistorical analysis of abnormal magnetic field under slow extantion of ocean bottom in Eurasian basin of the Arctic Ocean," in *Magnetic Anomalies of the Oceans and New Global Tectonics* (Nauka, Moscow, 1981), pp. 162–174.

8. B. I. Kim and Z. I. Glezer, "Sedimentary cover of the Lomonosov Ridge: Stratigraphy, structure, deposition history, and ages of seismic facies units," *Stratigr. Geol. Correl.* **15**, 401–420 (2007).
9. V. I. Kovalenko, V. V. Yarmolyuk, and O. A. Bogatkov, "The contemporary North Pangea supercontinent and the geodynamic causes of its formation," *Geotectonics* **44**, 448–461 (2010).
10. L. I. Lobkovskii, V. E. Verzhbitskii, M. V. Kononov, et al., "Geodynamic model of evolution of Arctic region in the late Mesozoic–Cenozoic and the problem of external boundary of continental shelf of Russia," *Arkt.: Ekol. Ekon.*, No. 1, 104–115 (2011).
11. V. A. Poselov, S. M. Zholonde, A. I. Trukhalev, et al., "A map of power of sedimentary layer of the Arctic Ocean," *Tr. Vseross. Nauchno-Issled. Inst. Geol. Miner. Resur. Mirovogo Okeana* **223** (8), 8–14 (2012).
12. S. Yu. Sokolov, "Tectonic elements of the Arctic region inferred from small-scale geophysical fields," *Geotectonics* **43**, 18–33 (2009).
13. N. I. Filatova and V. E. Khain, "The Arctida Craton and Neoproterozoic–Mesozoic orogenic belts of the Circum-Polar region," *Geotectonics* **44**, 203–227 (2010).
14. A. A. Chernykh and A. A. Krylov, "History of sedimentogenesis in the Amundsen depression according to geophysical data and drilling materials ACEX (IODP-302)," *Tr. Vseross. Nauchno-Issled. Inst. Geol. Miner. Resur. Mirovogo Okeana* **210**, 56–66 (2010).
15. A. A. Schreider, "Magnetism of the ocean crust and linear paleomagnetic anomalies," *Fiz. Zemli*, No. 6, 59–70 (1992).
16. A. A. Schreider, "Linear magnetic anomalies in the Arctic Ocean," *Oceanology (Engl. Transl.)* **44**, 721–729 (2004).
17. A. A. Schreider, "Model of the separation of the Marvin Spur from the Lomonosov Ridge in the Arctic Ocean," *Oceanology (Engl. Transl.)* **54**, 490–496 (2014).
18. V. E. Khain, *Tectonics of Continents and Oceans* (Nauchnyi Mir, Moscow, 2001) [in Russian].
19. A. Alvey, C. Gaina, N. Kuszner, and T. Torsvik, "Integrated crustal thickness mapping and plate reconstructions for the high Arctic," *Earth Planet. Sci. Lett.* **274**, 310–321 (2008).
20. J. Backman, K. Moran, D. B. McInroy, et al., *Proceedings of the Integrated Ocean Drilling Program* (Washington, 2006), Vol. 302.
21. Bathymetry Data Base, IBCAO, 2015. http://topex.ucsd.edu/html/mar_topo.html.
22. J. Brozena, V. Childers, L. Lawver, et al., "New aerogeophysical study of the Eurasian Basin and Lomonosov Ridge implications for basin development," *Geology* **31**, 825–828 (2003).
23. E. Bullard, J. Everett, and A. Smith, "The fit of the continents around the Atlantic," *Philos. Trans. R. Soc., A* **258**, 41–51 (1965).
24. V. Childers, D. McAdoo, J. Brozena, and S. Laxon, "New gravity data in the Arctic Ocean: Comparison of airborne and ERS gravity," *J. Geophys. Res.: Solid Earth* **106**, 8871–8886 (2001).
25. J. Cochran, M. Edwards, and B. Coakley, "Morphology and structure of the Lomonosov Ridge, Arctic Ocean," *Geochem., Geophys., Geosyst.* **7**, (2006).
26. R. Coles and P. Taylor, "Magnetic anomalies," in *Geology of North America* (Geological Society of America, Boulder, 1990), Vol. 1, pp. 119–132.
27. A. Dossing, H. Jackson, and J. Matzka, "On the origin of the Amerasia basin and the high Arctic large igneous province—results of new aeromagnetic data," *Earth Planet. Sci. Lett.* **363**, 219–230 (2013).
28. A. Dossing, L. Stemmerik, T. Dahl-Jensen, and V. Schlindwein, "Segmentation of the eastern north Greenland oblique shear margin—regional plate tectonic implications," *Earth Planet. Sci. Lett.* **292**, 239–253 (2010).
29. O. Engen, J. Gjengedal, J. Faleide, et al., "Seismic stratigraphy and sediment thickness of the Nansen basin, Arctic Ocean," *Geophys. J. Int.* **176**, 805–821 (2009).
30. O. Engen, J. I. Faleide, F. Tsikalas, et al., "Structure of the west and north Svalbard margins in a plate tectonic setting," in *Proceedings of the IV International Conference on Arctic Margins* (Dartmouth, 2003), p. 40.
31. O. Engen, J. Faleide, and T. Dyreng, "Opening of the Fram Strait gateway: a review of plate tectonic constraints," *Tectonophysics* **450**, 51–69 (2008).
32. C. Gaina, W. R. Roest, and R. D. Muller, "Late Cretaceous–Cenozoic deformation of northeast Asia," *Earth Planet. Sci. Lett.* **197**, 273–286 (2002).
33. W. Geissler and W. Jokat, "A geophysical study of the northern Svalbard continental margin," *Geophys. J. Int.* **158**, 50–66 (2004).
34. W. Geissler, W. Jokat, and H. Brekke, "The Yermak Plateau in the Arctic Ocean in the light of reflection seismic data—implication for its tectonic and sedimentary evolution," *Geophys. J. Int.* **187**, 1334–1362 (2011).
35. A. F. Grachev, "The Arctic rift system and the boundary between the Eurasian and North American lithospheric plates: new insight to plate tectonic theory," *Russ. J. Earth Sci.* **5**, 307–345 (2003).
36. F. Gradstein, J. Ogg, M. Schmitz, and G. Ogg, *The Geologic Timescale 2012* (Elsevier, Amsterdam, 2012).
37. A. Grantz, P. Hart, and V. Childers, "Geology and tectonic development of the Amerasia and Canada basins, Arctic Ocean," *Geol. Soc. Lond. Mem.* **35**, 771–799 (2011).
38. A. Grantz, R. Scott, S. Drachev, et al., "Sedimentary successions of the Arctic region (58°–64° to 90° N) that may be prospective for hydrocarbons," *Geol. Soc. Lond. Mem.* **35**, 17–37 (2011).
39. H. Jackson and G. Johnson, "Summary of arctic geophysics," *J. Geodyn.* **6**, 245–262 (1986).
40. H. Jackson and K. Gunnarson, "Reconstructions of the Arctic: Mesozoic to present," *Tectonophysics* **172**, 303–322 (1990).
41. H. Jackson, T. Dahl-Jensen, et al., "Sedimentary and crustal structure from the Ellesmere island and Greenland continental shelves onto the Lomonosov Ridge, Arctic Ocean," *Geophys. J. Int.* **182**, 11–35 (2010).
42. W. Jokat and U. Micksch, "The sedimentary structure of Nansen and Amundsen basins, Arctic Ocean,"

- Geophys. Res. Lett. **31**, L02603 (2004). doi 10.1029/2003/GL018352
43. W. Jokat, E. Weigelt, Y. Kristoffersen, et al., "New insights into the evolution of the LR and the Eurasian Basin," *Geophys. J. Int.* **122**, 378–392 (1995).
 44. W. Jokat, G. Uenzelmann-Neben, Y. Kristoffersen, and T. Rasmussen, "Lomonosov Ridge—a double-sided continental margin," *Geology* **20**, 887–890 (1992).
 45. S. Kashubin, O. Petrov, E. Andrusov, et al., "Crustal thickness in the circum arctic," in *Proceedings VI International Conference on Arctic Margins* (Fairbanks, 2011), pp. 1–18.
 46. L. Kovacks, C. Bernero, G. Johnson, et al., "Residual magnetic anomaly chart of the Arctic Ocean region," in *Geological Society of America Map Chart Series MC53, Scale 1 : 6000000* (Geological Society of America, Boulder, 1985).
 47. Y. Kristoffersen, "Eurasia Basin," in *Geology of North America* (Geological Society of America, Boulder, 1990), **Vol. 1**, pp. 365–378.
 48. Y. Kristoffersen and E. Husebye, "Multi-channel seismic reflection measurements in the Eurasian Basin, Arctic Ocean, from U.S. ice station FRAM-IV," *Tectonophysics* **114**, 103–115 (1985).
 49. Y. Kristoffersen and N. Mikkelsen, "On sediment deposition and nature of the plate boundary at the junction between the submarine Lomonosov Ridge, Arctic Ocean and the continental margin of Arctic Canada/North Greenland," *Mar. Geol.* **225**, 265–278 (2006).
 50. A. Langinen, N. Lebedeva–Ivanova, D. Gee, and Ya. Zamansky, "Correlation between the Lomonosov Ridge, Marvin Spur and adjacent basins of the Arctic Ocean based on seismic data," *Tectonophysics* **472**, 309–322 (2009).
 51. L. Lawver, A. Grantz, and L. Gahagan, "Plate kinematic evolution of the present Arctic region since the Ordovician," *Geol. Soc. Am. Spec. Pap.* **360**, 333–358 (2002).
 52. N. Lebedeva–Ivanova, PhD Dissertation (Uppsala Univ., Uppsala, 2010).
 53. D. C. McAdoo, S. L. Farrell, S. W. Laxon, et al., "Arctic Ocean gravity field derived from ICESat and ERS-2 altimetry: tectonic implications," *J. Geophys. Res.: Solid Earth* **113**, (2008).
 54. A. Minakov, J. Faleide, V. Glebovsky, and R. Mjelde, "Structure and evolution of the northern Barents-Kara sea continental margin from integrated analysis of potential fields, bathymetry and sparse seismic data," *Geophys. J. Int.* **188**, 79–102 (2012).
 55. K. Moran, J. Backman, H. Brinkhuis, et al., "The Cenozoic paleoenvironment of the Arctic Ocean," *Nature* **441**, 601–605 (2006).
 56. N. Okay and K. Crane, "Thermal rejuvenation of the Yermak Plateau," *Mar. Geophys. Res.* **15**, 243–263 (1993).
 57. G. Oakey and R. Stephenson, "Crustal structure of the Innuitian region of Arctic Canada and Greenland from gravity modeling: implications for the Palaeogene Eureka orogen," *Geophys. J. Int.* **173**, 1039–1063 (2008).
 58. W. C. Pitman and M. Talwani, "Sea-floor spreading in the North Atlantic," *Geol. Soc. Am. Bull.* **83**, 619–649 (1972).
 59. V. Poselov, V. Butsenko, A. Chernykh, et al., "The structural integrity of the Lomonosov Ridge with the north American and Siberian continental margins," in *Proceedings VI International Conference on Arctic Margins* (Fairbanks, 2011), pp. 233–268.
 60. O. Ritzmann and W. Jokat, "Crustal structure of north-western Svalbard and the adjacent Yermak Plateau: evidence for Oligocene detachment tectonics and non-volcanic breakup," *Geophys. J. Int.* **152**, 139–159 (2003).
 61. O. Ritzmann, W. Jokat, W. Czuba, et al., "A deep seismic transect from Hovgard Ridge to northwestern Svalbard across the continental-ocean transition: a sheared margin study," *Geophys. J. Int.* **157**, 683–702 (2004).
 62. S. Srivastava, "Evolution of the Eurasian Basin and its implications to the motion of Greenland along Nares Strait," *Tectonophysics* **114**, 29–53 (1985).
 63. P. Taylor, L. Kovacs, P. Vogt, and G. Johnson, "Detailed aeromagnetic investigations of the Arctic Basin: 2," *J. Geophys. Res.: Solid Earth* **86**, 6323–6333 (1981).
 64. M. Talwani and O. Eldholm, "Evolution of the Norwegian–Greenland Sea," *Geol. Soc. Am. Bull.* **88**, 969–999 (1977).
 65. M. Urlaub, M. Schmidt–Aursch, W. Jokat, and N. Kaul, "Gravity crustal models and heat flow measurements for the Eurasia basin, Arctic Ocean," *Mar. Geophys. Res.* **30**, 277–292 (2009).
 66. P. Vogt, "Magnetic anomalies and crustal magnetization," in *The Western North Atlantic Region* (Geological Society of America, Boulder, 1986), pp. 229–256.
 67. P. Vogt, P. Taylor, L. Kovacs, and G. Johnson, "Detailed aeromagnetic investigation of the Arctic Basin," *J. Geophys. Res.: Solid Earth* **84**, 1071–1089 (1979).
 68. E. Weigelt and W. Jokat, "Peculiarities of roughness and thickness of oceanic crust in the Eurasia Basin, Arctic Ocean," *Geophys. J. Int.* **145**, 505–516 (2001).
 69. B. Wernicke, "Low angle normal faults in the basin and range province: nappe tectonics in an extending orogeny," *Nature* **291**, 645–648 (1981).
 70. D. Winkelmann, W. Jokat, F. Niessen, et al., "Age and extent of the Yermak Slide north of Spitsbergen, Arctic Ocean," *Geochem., Geophys., Geosyst.* **7** (6), Q06007 (2006). doi 10.1029/2005GC001130
 71. USGS Earthquake Hazards Program, 2015. <https://earthquake.usgs.gov/>.

Translated by A. Carpenter